Issues of Soil Moisture Coupling in MM5: Simulation of the Diurnal Cycle over the FIFE Area

DYI-HUEY CHANG, LE JIANG, AND SHAFIQUL ISLAM

Cincinnati Earth Systems Science Program, Department of Civil and Environmental Engineering, University of Cincinnati, Cincinnati, Ohio

(Manuscript received 30 June 1999, in final form 25 June 2000)

ABSTRACT

This study evaluates the issues of soil moisture coupling on the partitioning of surface fluxes at the diurnal timescale over a mesoscale domain from the First International Satellite Land Surface Climatology Project Field Experiment (FIFE) in Kansas. A state-of-the-art atmospheric model (the Fifth-Generation Pennsylvania State University–National Center for Atmospheric Research Mesoscale Model, or MM5) is used as a control run in which soil moisture is prescribed by a time-invariant as well as time-varying moisture availability function. Then, in a coupled model simulation, the atmospheric model is coupled with a detailed land surface model. Three days are simulated with progressively smaller surface soil moisture conditions to identify the influence of interactive soil moisture on surface fluxes partitioning at the diurnal timescale. Preliminary results suggest that, for days with wetter surface soil moisture conditions and moderately high wind speed, a time-variant interactive soil moisture representation provides a more accurate partitioning of surface fluxes. For drier surface conditions with relatively low wind speed, a constant soil moisture availability function may be adequate.

1. Introduction

The moisture state of the land surface is a critical variable for various hydrological, meteorological, and ecological studies. It changes with the seasons and the dynamics of the storm and interstorm periods. The near-surface layer of the soil can switch between a source and a sink for moisture, depending on the antecedent surface and atmospheric conditions. The soil moisture state near the surface governs the surface and subsurface runoff, determines the extent of groundwater recharge, affects the partitioning of solar radiation into surface fluxes, and can initiate, modulate, and sustain interactions between land and atmosphere over a range of time- and space scales.

Hydrologists have used surface soil moisture states for partitioning precipitation into infiltration and runoff ever since Horton (1933) introduced the concept of overland flow. Namias (1958) was among the first in the meteorological community to address the influence of surface soil moisture anomalies on the atmospheric circulations at the seasonal scales. These pioneering studies have provided critical insight on the role of surface soil moisture states for surface and atmospheric processes. These studies, however, have not considered the interactive nature of the surface and the atmosphere. Horton (1933) and subsequent hydrologic studies have taken precipitation as a given atmospheric forcing, while Namias (1958) and subsequent atmospheric studies have examined the impact of prescribed soil moisture anomalies on the atmosphere.

Manabe (1969) was perhaps the first to introduce the concept of interactive soil moisture in general circulation models (GCMs) and has shown that interactive soil moisture has a significant influence on the temporal and spatial persistence of atmospheric processes. Since then several studies have examined the role of interactive soil moisture at various temporal and spatial scales. For example, it has been shown that changes in the soil moisture regime at the end of spring and beginning of summer can alter summer precipitation conditions over continental landmasses (Yeh et al. 1984; Pan et al. 1995). At the regional scale, Yang et al. (1995) tested the forecast errors of 5- and 10-day integrations of a numerical weather prediction model with various initializations of the soil moisture state. In contrast to several studies examining effects of soil moisture on continental and regional scales on timescales of days to seasons, little effort has been made to examine the effects of interactive soil moisture coupling at the diurnal scale within a coupled land–atmosphere system.

Two general approaches are usually employed to represent temporal change of soil moisture at the land sur-

Corresponding author address: Dr. Shafiqul Islam, Cincinnati Earth Systems Science Program, P.O. Box 210071, University of Cincinnati, Cincinnati, OH 45221-0071.
E-mail: shafiqul.islam@uc.edu

face. The first approach does not use any prognostic equations for soil moisture dynamics but uses empirical relationships to calculate soil flux near the surface (e.g., Pielke 1984; Deardorff 1978). Because of their relative simplicity, variants of this approach are widely used in operational weather forecast and climate models. The second approach, on the other hand, uses a multilayer soil moisture with explicit prognostic equations for heat and moisture transport in the soil. Consequently, the second approach is more responsive to short-term changes in surface and atmospheric conditions. This approach, however, requires additional soil-related parameters and computational resources. As a result, use of this class of models has been largely confined within the research community models (e.g., McCumber and Pielke 1981; Noilhan and Planton 1989). Recently, Viterbo and Beljaars (1995) incorporated a four-layer detailed land surface scheme in the European Centre for Medium-Range Weather Forecasts (ECMWF) model. They have shown that this representation of soil moisture dynamics captures a wide range of timescales, from diurnal to seasonal to interannual scales, and improves the model performance significantly.

Because global-scale models such as the ECMWF model typically have a horizontal grid resolution on the order of 100 km, they are not particularly suitable for studying effects of interactive soil moisture coupling at the diurnal scale. This is partly because most of the small-scale variability important for diurnal soil moisture dynamics occurs at a scale much finer than 100 km. The Fifth-Generation Pennsylvania State University–National Center for Atmospheric Research Mesoscale Model, popularly known as MM5, is a state-of-the-art, three-dimensional, finite-difference atmospheric model capable of simulating both hydrostatic and nonhydrostatic conditions [see Dudhia (1993) and Grell (1993), and references therein]. MM5 has been used extensively to investigate various mesoscale phenomena (e.g., Grell 1993; Oncley and Dudhia 1995).

Although many aspects of MM5 have been significantly improved, soil moisture and surface flux parameterizations are based on studies done almost two decades ago (Deardorff 1978; Carlson and Boland 1978). Recently, several studies attempted to couple detailed land surface models with the previous version of MM (e.g., Giorgi and Marinucci 1996) and MM5 (e.g., Pleim and Xiu 1995). A popular version of MM5 uses an empirical soil moisture availability function to specify time-invariant soil moisture content for different land types. Such a function usually takes the seasonally averaged surface soil moisture value for each land type and neglects the temporal evolution of soil moisture during the model integration period. It is argued that because surface processes are generally slower than atmospheric boundary layer processes, land surface variables like soil moisture may be viewed as integrators of atmospheric processes and can be taken as constant for shorter-timescale integration. An implication of this assertion is that simplified empirical parameterizations of soil moisture would be adequate for short timescale integration of coupled land–atmosphere models. Several stand-alone (i.e., not coupled with an atmospheric model) modeling studies suggest that a short-timescale change in soil moisture may have significant effects on the partitioning of surface fluxes, depending on the antecedent soil moisture states (Wood 1991).

A key objective of this study is to examine the importance of interactive soil moisture coupling in simulating the partitioning of surface fluxes and other near-surface variables at the diurnal timescale. We will compare and contrast results of three simulations of MM5 in its original mode (i.e., noninteractive soil moisture) and coupled mode (i.e., interactive soil moisture). Comparison of these simulations with observed datasets from the First International Satellite Land Surface Climatology Project Field Experiment (FIFE) is expected to provide insight on the importance of interactive soil moisture dynamics at the diurnal timescale. By studying the diurnal cycle for several cloud-free days with a range of initial soil moisture conditions, we plan to identify signatures of improvement in the partitioning of fluxes due to corresponding improvement in the coupling between soil moisture states and atmospheric dynamics.

2. Model description and coupling issues

a. Atmospheric model—MM5

The atmospheric module of our coupled model is the nonhydrostatic version of MM5. MM5 is based on a fully compressible atmosphere in a rotating frame of reference, including terrain-following coordinates and a split semi-implicit temporal integration scheme. This is a well-studied, state-of-the-art mesoscale model designed to support basic atmospheric research and it has wide community support for further developments and refinements for a range of hydrometeorological applications. Various developments, physical parameterizations, and numerical techniques are described in the literature [see Anthes and Warner (1978), Dudhia (1993), Grell (1993), and references therein] and will not be repeated here.

This atmospheric model is a primitive equation model that solves a simultaneous set of eight nonlinear prognostic equations in the eight dependent variables (pressure perturbation, temperature, three components of velocity, water vapor, cloud water, and rain water). The model equations are described within a vertically stretched system. Also, the techniques of successive one-way nesting allows one to dynamically feed synoptic-scale features down to cloud scales.

Currently, MM5 uses multilayer Blackadar planetary boundary layer parameterizations to represent turbulent fluxes of heat, moisture, and momentum (Zhang and Anthes 1982). We note that although certain aspects of MM5 have been greatly improved over earlier versions,

a popular version of the land surface parameterization is based on two studies—Deardorff (1978) and Carlson and Boland (1978)—done 18 years ago (Oncley and Dudhia 1995). Previous studies, however, have shown that the surface flux parameterizations used in earlier MM5 work reasonably well for long-term simulations, given appropriate values of required parameters (Oncley and Dudhia 1995). These parameters include albedo α, soil moisture availability M, surface emissivity ε, roughness length z_0, and thermal inertia λ_T. Currently, MM5 assigns constant values for these parameters based on 13 land-use categories. Oncley and Dudhia (1995) demonstrated that surface fluxes are quite sensitive to M. They suggested either to assume that the value of M is equal to the initial surface-layer soil moisture or to run MM5 iteratively to find the proper value of M. A key objective of this study is to explore the sensitivity of interactive soil moisture dynamics at a diurnal cycle. We will use MM5 in its original mode (with a time-invariant as well as time-varying soil moisture availability function) and in its coupled mode. In the coupled mode, we will couple a four-layer land surface model (described in section 2b) with MM5 in its nonhydrostatic mode with one of its high-resolution planetary boundary layer schemes, to simulate the diurnal cycle.

b. Land surface model

The land surface model used in this study is a variant of the land surface model developed by Viterbo and Beljaars (1995) for the ECMWF model. It is designed to compute different components of the surface energy and moisture budget over different land surfaces. Surface parameterizations are derived from Deardorff (1977, 1978), Abramopoulous et al. (1988), Hu and Islam (1995), and Viterbo and Beljaars (1995). Particular attention is given to capturing the principal physical mechanisms through a minimum number of parameters. Important features of the model are highlighted below.

- The surface heat and moisture budgets are represented by two partial differential equations (assuming snow-free ground). The total soil depth, number of layers, and boundary conditions are chosen such that all relevant timescales, ranging from diurnal cycles to seasonal cycles, are adequately represented.
- It uses an improved version of the discretization method for soil heat and moisture content. This improvement is achieved by minimizing the error produced by the force–restore approximation of the diffusion equation (Hu and Islam 1995).
- The evaporation rate from the canopy and from the bare soil consists of three components: evaporation of water from the wetted canopy, transpiration of soil water extracted by the root system, and evaporation from the bare soil.
- Soil hydraulic and thermal properties are characterized by using the Clapp and Hornberger (1978) and McCumber and Pielke (1981) formulations.

This land surface model has four soil layers, and each layer treats soil moisture movement with different timescales. Qualitatively, the first layer represents the diurnal cycle, the second layer represents variations between 1 day and 1 week, the third layer represents variations between 1 week and 1 month, and the fourth layer varies with timescales larger than 1 month. In addition to the four soil layers, there is a skin layer at the top that has no heat capacity and is in instantaneous equilibrium with atmospheric forcing, which allows quick response to the atmospheric condition change at the top. The depths of soil layer are taken in an approximate geometric relation as suggested by Deardorff (1978) and adopted by Viterbo and Beljaars (1995). It has been shown that four layers are sufficient to capture soil moisture dynamics from diurnal to seasonal cycles (Warrilow et al. 1986) The soil heat and moisture transfer are described by classical diffusion equations. The top boundary conditions are obtained from solution of the surface moisture and energy balance equations, and the heat and moisture fluxes from the bottom of the fourth layer are taken to be zero. The thermal diffusivity and moisture diffusivity are parameterized as a function of soil moisture and temperature (Clapp and Hornberger 1978). The surface temperature is computed from the surface energy balance equation:

$$\Lambda_{\rm sk}(T_{\rm sk} - T_1) = (1 - \alpha)R_S + (R_T - \varepsilon\sigma T_{\rm sk}^4) + H_s + \text{LE}, \quad (1)$$

where $\Lambda_{\rm sk}$ is skin layer conductivity, $T_{\rm sk}$ is surface temperature, T_1 is first-layer soil temperature, R_S is downward shortwave radiation, R_T is downward longwave radiation, σ is the Stefan–Boltzmann constant, H_s is sensible heat flux, and LE is latent heat flux. The sensible and latent heat fluxes are parameterized as

$$H_s = \rho C_H|V|(C_pT_L + gZ_L - C_pT_{\rm sk}) \quad \text{and} \quad (2)$$

$$\text{LE} = \rho C_H|V|[a_Lq_L - a_Sq_{\rm sat}(T_{\rm sk}, p_s)], \quad (3)$$

where ρ is air density, C_H is heat transfer coefficient, C_P is heat capacity of air at constant pressure, g is acceleration due to gravity, Z_L is the height of the lowest atmospheric layer, $q_{\rm sat}$ is the saturated specific humidity, and p_s is surface pressure. Also, $|V|$, T_L, and q_L are the wind speed component, atmosphere temperature, and specific humidity at the lowest atmospheric layer, respectively.

The surface temperature $T_{\rm sk}$ is solved from Eqs. (1) through (3) by obtaining the forcing data (R_s, R_T, $|V|$, T_L, q_L, p_s, Z_L, and precipitation) from the atmospheric module of MM5. The resulting $T_{\rm sk}$, LE, and H_s are then fed back to the land surface boundary condition of MM5. The first-layer soil temperature is obtained from a difference equation representing the soil heat budget. In Eq. (3) the constants a_L and a_S are related to moisture

availability function. In ECMWF, a_L and a_S are implicitly defined for three fractions of total evaporation: 1) fraction covered by the interception reservoir E_I, 2) vegetation fraction E_V, and 3) bare soil fraction E_B. The total evaporation is a linear combination of these three components. Because more than 85% of the FIFE area is covered by vegetation, we only describe the constants a_L and a_S defined in E_V:

$$a_L = a_S = \frac{r_a}{r_a + r_c}. \tag{4}$$

Variables r_a and r_c are aerodynamic resistances:

$$r_a = \frac{1}{C_H|V|} \quad \text{and} \tag{5}$$

$$r_c = \frac{r_{\text{smin}}}{L_f} f_1(\text{PAR}) f_2(\theta), \tag{6}$$

where

$$\frac{1}{f_1(\text{PAR})} = 1 - a_1 \log\frac{a_2 + \text{PAR}}{a_3 + \text{PAR}}, \quad \text{and} \tag{7}$$

$$\frac{1}{f_2(\overline{\theta})} = \begin{cases} 0 & \overline{\theta} < \theta_{\text{pwp}} \\ \dfrac{\overline{\theta} - \theta_{\text{pwp}}}{\theta_{\text{cap}} - \theta_{\text{pwp}}} & \theta_{\text{pwp}} \le \overline{\theta} \le \theta_{\text{cap}} \\ 1 & \overline{\theta} > \theta_{\text{cap}}. \end{cases} \tag{8}$$

Here r_{smin} is minimum stomatal resistance of a single leaf, L_f is leaf area index, PAR is photosynthetically active radiation, θ is soil moisture, θ_{pwp} is soil moisture at permanent wilting point, θ_{cap} is soil moisture at field capacity, $\overline{\theta}$ is average soil moisture, and a_1, a_2, and a_3 are related to canopy properties (Sellers 1985). In Eqs. (6) and (8), the soil moisture is obtained from a difference equation representing the soil water budget. For a detailed description of this land surface model, we refer the reader to Viterbo and Beljaars (1995).

We have performed a detailed validation of this land surface model using the FIFE data (Li and Islam 1999). We highlight some of the findings of model validation here. The soil moisture for the first two layers is simulated well by the model. There may be a slight underestimation bias for the deeper layers. The latent heat flux is modeled well, with a correlation coefficient of 0.92, a positive bias of 10.3 W m^{-2}, and a root-mean-square error of 20.87 W m^{-2}. Sensible heat flux, on the contrary, has a bias of -22.14 W m^{-2}, a correlation coefficient of 0.65, and a root-mean-square error of 31.06 W m^{-2}. Viterbo and Beljaars (1995) have also done an extensive validation for this model for a range of surface and climate conditions, including the FIFE in the United States, Cabauw in the Netherlands, and the Amazonian Rainforest Meteorological Experiment in the central Amazonia. A version of this land surface model is currently used as a host land surface model within the ECMWF model.

c. Land–atmosphere coupling

Two methods will be used to couple a land surface model with an atmospheric model: 1) *control run*, in which surface fluxes are computed using the original MM5 in which soil moisture is prescribed through a moisture availability function; and 2) *coupled model*, in which the land–atmosphere fluxes respond to dynamic space–time changes in both the atmospheric and land surface variables. These two different ways of coupling are used to design experiments and successively to identify strength of land–atmosphere interactions within a coupled land–atmosphere modeling environment. For each day, we will use three different representations of soil moisture availability function M for the control-run simulations: control 1, for which M is equal to a constant soil moisture; control 2, for which M is equal to a constant following Kondo and Saigusa (1990) parameterizations; and control 3, for which M is equal to time-varying soil moisture following Kondo and Saigusa (1990) parameterizations. Here, M is defined as follows:

$$M_{(\text{Kondo})} = \frac{1}{1 + C_H|V|F(\theta)/D_{\text{atm}}}, \tag{9}$$

where $F(\theta)$ is a decreasing function of soil moisture that also depends on soil types, and D_{atm} is an increasing function of surface temperature. Although Kondo and Saigusa's (1990) parameterization of moisture availability function [$M_{(\text{Kondo})}$] is only applicable for bare soil, the parametric form of $M_{(\text{Kondo})}$ is somewhat similar to ECMWF's parameterization of moisture availablity function [$M_{(\text{ECMWF})}$], derived from Eqs. (3)–(6) as follows:

$$M_{(\text{ECMWF})} = \frac{1}{1 + C_H|V|r_c}, \tag{10}$$

where r_c, similar to $F(\theta)$, is a decreasing function of soil moisture that depends on soil types but also considers the influence of vegetation [see Eq. (6)]. Given that FIFE is 85% vegetated, it is likely that the coupled MM5–ECMWF model would provide more realistic results.

3. Design of experiments

a. Domain description and model specifications

We will simulate three cloud-free days: 15 August, 11 July, and 11 October from the FIFE 1987 near Konza prairie in Kansas. Our choice of days with no precipitation and little or no cloud allows us to use much simpler physics schemes (e.g., cloud scheme, radiation scheme, etc.) in the atmospheric part of the coupled model. This choice would also have minimal impact for simplified representation of land surface runoff and groundwater movement. These three days have a progressively smaller amount of surface soil moisture.

A 205 km $\times$ 205 km domain centered at the FIFE

site (39.05°N, 96.53°W) is simulated with a medium-resolution grid ($DX = DY = 5$ km). There are nine model grids at the center of the simulation domain covering the FIFE site (15 km × 15 km). Lateral boundary conditions are obtained from the National Centers for Environmental Prediction (NCEP) reanalysis products for the corresponding periods. A similar three-dimensional domain with time-dependent lateral boundary conditions has been used successfully to compare simulated data with the collected dataset from the Hydrological Atmospheric Pilot Experiment site (Bougealt et al. 1991). Use of the NCEP reanalysis data allows us to provide time-dependent lateral boundary conditions over the FIFE area.

The initial and boundary conditions for the model simulation are from the NCEP reanalysis archive. For both the control and coupled model simulations, the Grell cumulus parameterization (Grell 1993) is used. For the control run (i.e., MM5 in its original mode, with a prescribed soil moisture availability function), surface properties such as albedo, roughness length, and heat capacity are specified according to one of the 13 land use categories. The moisture availability is specified in three different ways, as described above, using FIFE domain observations of surface volumetric soil moisture, which are 0.300 for 15 August 1987, 0.235 for 11 July 1987, and 0.139 for the dry case of 11 October 1987. For the coupled model simulation, the spatial distribution of soil texture is obtained from a lookup table with seven soil classes based on Zobler (1986). These seven soil classes are then reclassified into three soil classes: coarse, medium, and fine. Soil properties for these three classes are derived from Patterson (1990). The vegetation fraction is set as 0.85 following Viterbo and Beljaars (1995).

b. Metrics for comparison

Because several kinds of sensors and measurement techniques were used to collect surface data for the relatively small FIFE area, a random error (due to different sensors and measurement techniques) is expected to be present in the observations (Betts and Ball 1993). It is conceivable that random errors due to numerical diffusion and turbulence parameterizations could also arise in the simulations for the FIFE area. To minimize the effects of such random errors, we plan to compare statistical moments of the observed mean time series data and the control and coupled model outputs over the FIFE area. Betts and Ball (1993) successfully used similar mean time series data for the FIFE 1987 data to detect systematic errors in the ECMWF model.

To compare the model simulation results with the 30-min-averaged FIFE observation series, we take 30-min-averaged values of the model output quantities and further average the model output quantities over the model grids covering FIFE site. The mean, correlation coefficient, and bias are calculated for the following variables: net radiation Rn, ground heat flux G, sensible heat flux H, LE, evaporative fraction [LE/(H + LE)], mixing ratio q, and surface wind speed U and V.

4. Results

We simulate three cloud-free days from the FIFE 1987 with progressively smaller surface soil moisture. The model simulation time is chosen as the FIFE site local daytime period, that is, 0600–1800 local time (corresponding to 1200–2400 UTC). In each case, the model is integrated for 12 h, from 0600 to 1800 local time. We will compare and contrast three simulations (with different soil moisture representations) of control-run and coupled-model simulations with observations over the entire 12-h simulation period. As indicated earlier, model output is averaged over 30-min intervals, as well as over the FIFE area, to facilitate comparison with the FIFE area-average observed datasets.

a. Wet case—15 August 1987

Fifteen August is a cloud-free day during the Intensive Field Campaign—3 (IFC-3). On this day, net radiation averaged over a 12-h period was 392.10 W m^{-2}. There was about 80 mm of precipitation over the FIFE area on 12–13 August 1987, which resulted in a volumetric soil moisture as high as 0.30. Because the land surface soil water content is usually replenished by precipitation and the soil moisture drydown period lasts for several days, this day may be considered to be the beginning of a drydown period. On this day, the average surface wind velocity was 8.0 m s^{-1}, and the mixing ratio was 17.5 g kg^{-1}.

Figures 1a,b show net radiation and ground heat flux simulated by the three control simulations and the coupled model. The net radiation is simulated well by both models. It appears, however, that control 1 is slightly better than the control-2 and control-3 simulations. Root-mean-square error (rmse) and the bias are comparable for both the control and coupled-model simulations. For the ground heat flux, the coupled model shows greater bias when compared with the control run.

Figures 1c,d show the sensible and latent heat fluxes for the control and coupled model simulations. The statistical metrics are comparable for the control-1 and coupled-model simulations, while the control-2 and control-3 simulations yield a very high bias and root-mean-square error for latent heat flux. Table 1 compares statistical metrics for several variables for all the simulations. In terms of bias and rmse, the coupled model, in general, gives better results in simulating H, LE, q, U, and V.

Several points are worth noting from these figures and Table 1. First, in Figs. 1a and 1b, simulation of net radiation by the control (particularly Control 1) and coupled model are similar and they agree well with observations. Second, in Figs. 1c and 1d, better partitioning

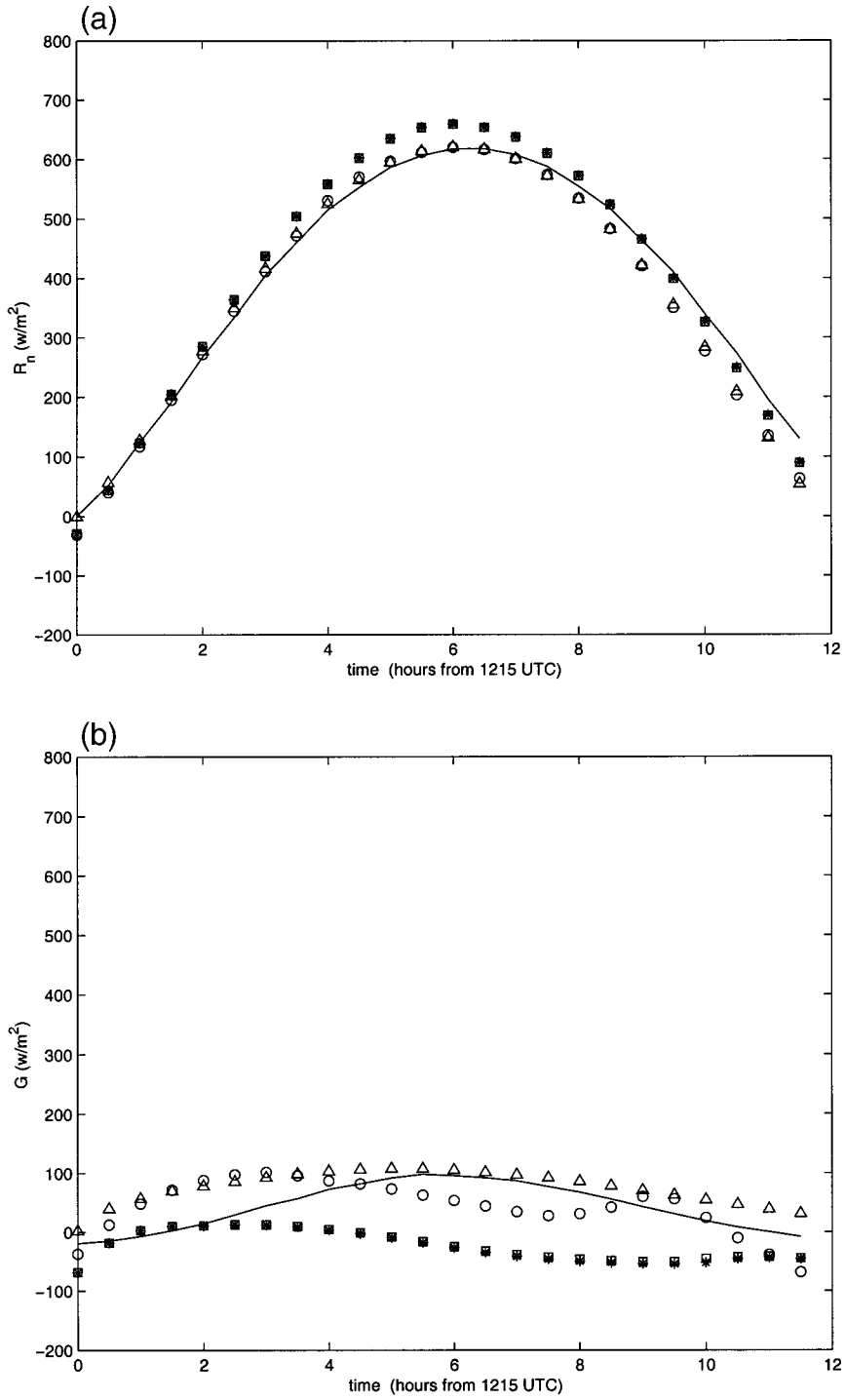

FIG. 1. Results for 12-h simulation starting at 0600 LT 15 Aug 1987: (a) net radiation, (b) ground heat flux, (c) sensible heat flux, and (d) latent heat flux. Solid line: FIFE observation; circle: control-1 simulation (original MM5 with constant $M = 0.30$); asterisk: control-2 simulation

between sensible heat flux and latent heat flux is achieved by the coupled model around the local noon time (6 h after model starts), at which time the control runs overestimate the latent heat flux and underestimate the sensible heat flux. Because the simulated wind components ($|U_L|^2 = u^2 + v^2$) are similar for all the simulations, one may argue that differences in surface fluxes for the control run are not due to errors in surface wind.

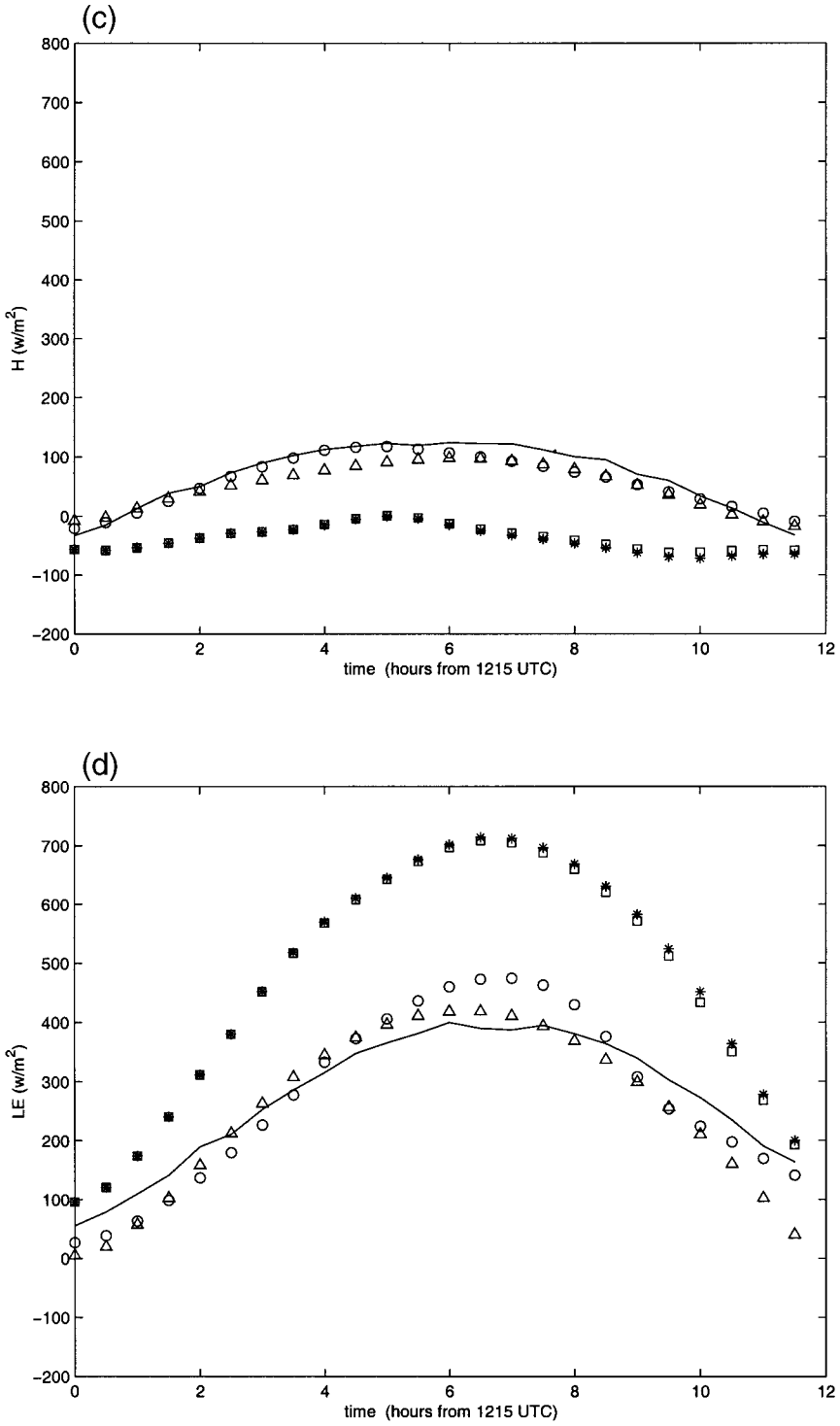

FIG. 1. (*Continued*) [original MM5 with constant *M* according to Kondo and Saigusa (1990)]; square: control-3 simulation [MM5 model with time-varying *M* according to Kondo and Saigusa (1990)]; triangle: coupled-model simulation.

TABLE 1. Comparison of model simulations with observations 1215–2345 UTC 15 Aug 1987.

Variable	Mean $\overline{X}_{\text{model}}$	Bias $\overline{X}_{\text{model}} - \overline{X}_{\text{obs}}$	Rmse
Original MM5 with constant $M = 0.30$ (control 1)			
Rn (W m^{-2})	376.0	−16.1	32.5
G (W m^{-2})	40.0	−2.3	44.1
H (W m^{-2})	48.1	−18.4	28.6
LE (W m^{-2})	287.8	14.7	59.1
LE/(H + LE)	0.8371	0.0421	0.0692
q (kg kg^{-1})	0.0193	0.0018	0.0033
U (m s^{-1})	0.86	0.11	1.29
V (m s^{-1})	6.34	−0.69	1.55
Original MM5 with constant M according to Kondo and Saigusa (1990) (control 2)			
Rn (W m^{-2})	406.1	14.0	30.5
G (W m^{-2})	−25.2	−67.5	81.1
H (W m^{-2})	−40.3	−26.3	113.7
LE (W m^{-2})	471.6	198.5	220.4
LE/(H + LE)	0.8898	0.0948	0.1645
q (kg kg^{-1})	0.0202	0.0028	0.0033
U (m s^{-1})	0.93	0.17	0.83
V (m s^{-1})	7.07	0.04	0.78
MM5 with time-varying M according to Kondo and Saigusa (1990) (control 3)			
Rn (W m^{-2})	405.6	13.5	30.4
G (W m^{-2})	−23.4	−65.8	79.1
H (W m^{-2})	−37.1	−29.5	110.6
LE (W m^{-2})	466.1	193.0	215.1
LE/(H + LE)	0.8942	0.0992	0.1654
q (kg kg^{-1})	0.0203	0.0028	0.0033
U (m s^{-1})	0.92	0.17	0.83
V (m s^{-1})	7.04	0.01	0.82
Coupled MM5–ECMWF model			
Rn (W m^{-2})	378.3	−13.7	32.5
G (W m^{-2})	75.3	32.9	37.6
H (W m^{-2})	50.3	−16.3	23.0
LE (W m^{-2})	252.8	−20.3	47.5
LE/(H + LE)	0.8134	0.0184	0.0752
q (kg kg^{-1})	0.0162	−0.0013	0.0028
U (m s^{-1})	0.12	−0.64	0.95
V (m s^{-1})	7.28	0.25	0.68

TABLE 2. Comparison of model simulation with observations 1215–2345 UTC 11 Jul 1987.

Variable	Mean $\overline{X}_{\text{model}}$	Bias $\overline{X}_{\text{model}} - \overline{X}_{\text{obs}}$	Rmse
Original MM5 with constant $M = 0.235$ (control 1)			
Rn (W m^{-2})	418.7	17.8	37.6
G (W m^{-2})	58.9	16.7	47.4
H (W m^{-2})	156.9	92.4	105.0
LE (W m^{-2})	202.9	−88.5	95.0
LE/(H + LE)	0.5839	−0.2470	0.2571
q (kg kg^{-1})	0.0168	−0.0003	0.0017
U (m s^{-1})	1.09	−0.48	1.41
V (m s^{-1})	8.21	−1.00	1.28
Original MM5 with constant M according to Kondo and Saigusa (1990) (control 2)			
Rn (W m^{-2})	449.5	48.6	60.2
G (W m^{-2})	−33.0	−75.3	88.4
H (W m^{-2})	−31.1	−33.5	102.1
LE (W m^{-2})	513.6	222.2	242.6
LE/(H + LE)	0.9202	0.0894	0.1558
q (kg kg^{-1})	0.0183	0.0012	0.0014
U (m s^{-1})	1.40	−0.16	0.45
V (m s^{-1})	8.82	−0.39	0.06
MM5 model with time-varying M according to Kondo and Saigusa (1990) (control 3)			
Rn (W m^{-2})	446.5	45.6	57.2
G (W m^{-2})	−22.4	−64.7	76.8
H (W m^{-2})	−12.9	−51.7	86.1
LE (W m^{-2})	481.8	190.4	209.3
LE/(H + LE)	0.9425	0.1117	0.1618
q (kg kg^{-1})	0.0184	0.0013	0.0015
U (m s^{-1})	1.35	−0.21	0.51
V (m s^{-1})	8.68	−0.54	0.80
Coupled MM5–ECMWF model			
Rn (W ms^{-2})	427.2	26.3	42.5
G (W m^{-2})	32.9	−9.4	43.9
H (W m^{-2})	97.1	32.6	36.8
LE (W m^{-2})	297.2	5.8	42.2
LE/(H + LE)	0.7624	−0.0685	0.0826
q (kg kg^{-1})	0.0178	0.0007	0.0016
U (m s^{-1})	0.99	−0.58	1.30
V (m s^{-1})	8.13	−1.08	1.36

To understand the primary cause for differences in surface flux partitioning, one needs to look at the diurnal dynamics of soil moisture. The top-layer (0–7 cm) soil moisture drydown simulated by the coupled model shows a monotonic depletion of surface soil moisture from 0.30 to 0.25, but in the control-1 simulation soil moisture is kept at a constant value of 30%. This diurnal reduction in moisture availability is not considered in the control run, which consequently results in an overestimation of latent heat flux. For the control-2 and control-3 simulations, on the other hand, latent heat flux is overestimated because of the nonlinear relationship, proposed by Kondo and Saigusa (1990), between soil moisture availability function and soil moisture content. Results from the three control simulations demonstrate the sensitivity of specifying M in controlling the partitioning of surface fluxes. Note that, despite a reasonable simulation of net radiation, control simulations fail to reproduce accurate partitioning of surface fluxes because of inaccurate representation of soil moisture dynamics.

b. Moderate wet case—1987 July 11

Eleven July is another cloud-free day during the IFC-2. Net radiation averaged over a 12-h period was 400.90 W m^{-2}, and the 6-h peak average net radiation was 552 W m^{-2}. The observed soil moisture was 0.24, and the average surface wind speed and mixing ratio were 8.2 m s^{-1} and 17.10 g kg^{-1}. In terms of average net radiation, ground heat flux, mixing ratio, and wind speed, this day is similar to 15 August 1987. Surface soil moisture, however, was lower on this day.

Table 2 compares performance of three control and coupled-model simulations. The net radiation is simulated well by both the models. Root-mean-square error, correlation between observed and model, and the bias are comparable for both the control-1 and coupled-mod-

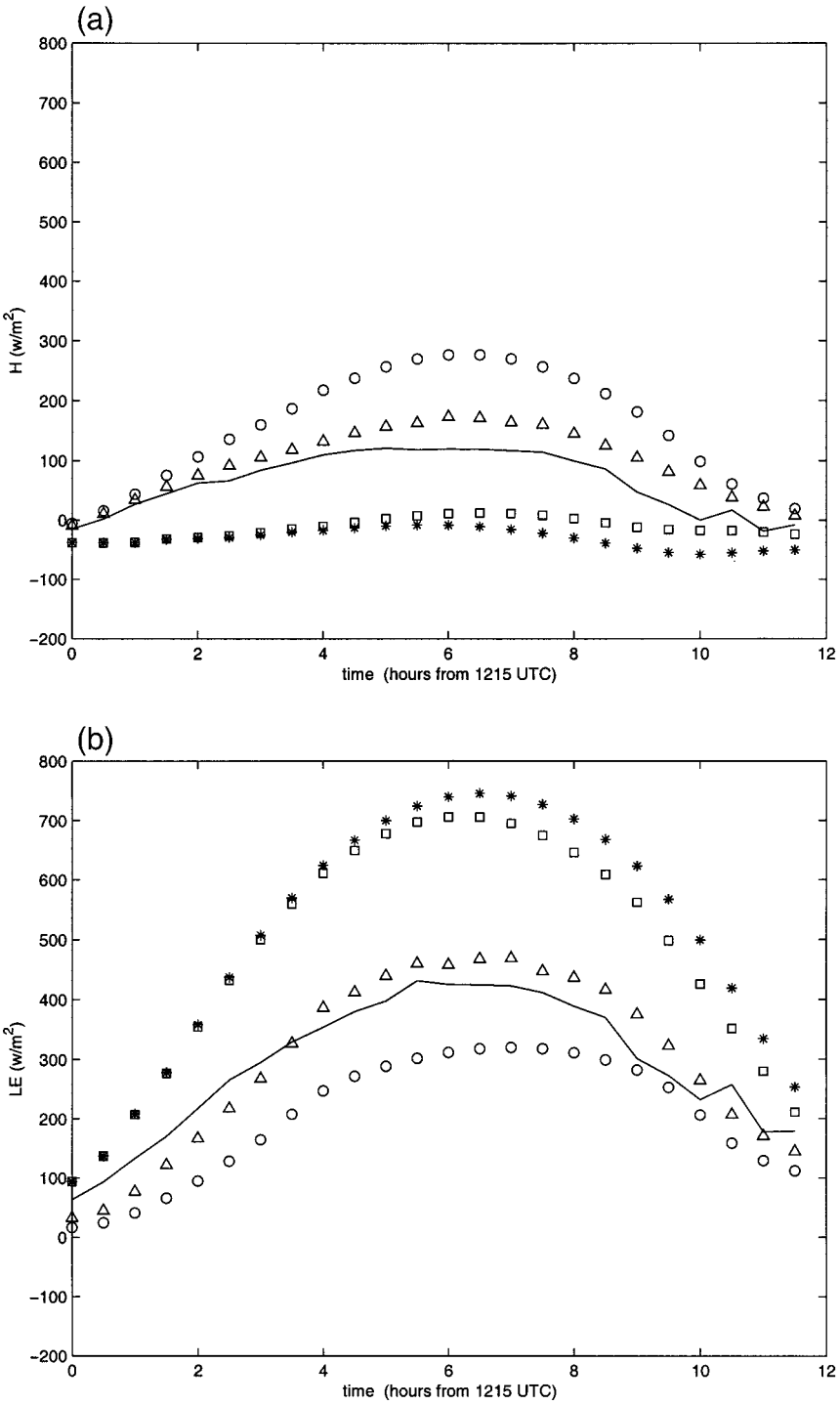

FIG. 2. (a) Sensible and (b) latent heat fluxes for 12-h simulation starting at 0600 LT 11 Jul 1987. Symbols are defined as in Fig. 1.

el simulations. For the ground heat flux, the coupled model shows small bias; control 2 and control 3 show significant bias and large rmse. The correlation coefficient between the observed and simulated ground heat flux is low for all the simulations. Figures 2a,b show the sensible and latent heat fluxes for the control and coupled-model simulations. There is a large bias in the partitioning of fluxes for the control simulations, but the coupled model has provided a fairly accurate partitioning of radiative forcing into sensible and latent heat

TABLE 3. Comparison of model simulation with observations 1215–2345 UTC 11 Oct 1987.

Variable	Mean $\overline{X}_{\text{model}}$	Bias $\overline{X}_{\text{model}} - \overline{X}_{\text{obs}}$	Rmse
Original MM5 with constant $M = 0.139$ (control 1)			
Rn (W m^{-2})	238.7	18.8	43.4
G (W m^{-2})	65.9	55.1	76.1
H (W m^{-2})	140.0	−35.0	44.2
LE (W m^{-2})	32.8	2.7	11.7
LE/(H + LE)	0.2497	0.0103	0.2369
q (kg kg^{-1})	0.0031	0.0000	0.0001
U (m s^{-1})	0.75	−0.25	0.57
V (m s^{-1})	−0.63	−0.49	0.60
Original MM5 with constant M according to Kondo and Saigusa (1990) (control 2)			
Rn (W m^{-2})	209.7	−10.3	30.7
G (W m^{-2})	55.1	44.3	69.2
H (W m^{-2})	124.2	−50.8	59.5
LE (W m^{-2})	30.3	0.2	10.0
LE/(H + LE)	0.2302	−0.0092	0.2244
q (kg kg^{-1})	0.0031	0.0000	0.0001
U (m s^{-1})	0.63	−0.36	0.64
V (m s^{-1})	−0.51	−0.38	0.50
MM5 model with time-varying M according to Kondo and Saigusa (1990) (control 3)			
Rn (W m^{-2})	209.2	−10.8	30.8
G (W m^{-2})	56.5	45.7	70.4
H (W m^{-2})	126.5	−48.5	57.6
LE (W m^{-2})	26.2	−3.9	7.2
LE/(H + LE)	0.2042	−0.0352	0.2136
q (kg kg^{-1})	0.0031	0.0000	0.0001
U (m s^{-1})	0.64	−0.36	0.64
V (m s^{-1})	−0.52	−0.38	0.50
Coupled MM5–ECMWF model			
Rn (W m^{-2})	150.4	−69.5	79.7
G (W m^{-2})	64.1	53.4	73.6
H (W m^{-2})	74.8	−100.2	111.5
LE (W m^{-2})	11.5	−18.6	20.2
LE/(H + LE)	0.0858	−0.1536	0.3000
q (kg kg^{-1})	0.0029	−0.0002	0.0003
U (m s^{-1})	−0.02	−1.02	1.41
V (m s^{-1})	−0.43	−0.29	0.58

fluxes. For example, control 1 produced a negative bias of 88.5 W m^{-2} for latent flux, and control 2 and control 3 yielded a positive bias of approximately 200 W m^{-2}. On the other hand, the coupled model has a bias of only 5.8 W m^{-2} for latent heat flux.

For other quantities, such as mixing ratio and surface wind speed, similar results are obtained by both the control run and the coupled model. Based on the results of 15 August and 11 July, one may argue that a detailed coupling between land surface soil moisture and atmosphere is important under moderately wet land surface conditions.

c. Dry case—11 October 1987

On 11 October 1987 (a cloud-free day from IFC-4), a high pressure system was over the domain for the simulation period. The average surface wind speed was very low—1–2 m s^{-1}. The boundary layer was dry over the FIFE observation domain (mixing ratio is about 3.1 g kg^{-1}) and the sky was clear to partly cloudy. Them was only a small amount (~2 mm) of precipitation during the previous day. The observed surface volumetric soil moisture content was about 0.14.

In this dry-case simulation, the surface latent heat flux was very small. Both the control and the coupled model underestimated the surface sensible flux, but the coupled model has a much larger bias. This bias is partly due to the large underestimation of net radiation by the coupled model. However, the correlation coefficients for surface fluxes are reasonably good from both model simulations (Table 3). The correlation coefficients for mixing ratio and surface wind (U and V) are also better for the control run. Overall, the results for this dry day show that the control run performs better than the coupled model in simulating daytime surface fluxes, mixing ratio, and surface wind speed. These results suggest that, for drier surface conditions, it may not be necessary to include a time-variant soil moisture representation for a coupled land–atmosphere model.

To isolate the influence of underestimation of net radiation on the land surface model, we have performed another simulation for 11 October 1987. In this simulation, the land surface model (described in section 2b) is integrated in its stand-alone mode. In other words, forcing for the land surface model (i.e., net radiation, wind speed, mixing ratio, etc.) is provided from the observed dataset. Figure 4 shows the time sequence of sensible and latent heat fluxes simulated by the stand-alone land surface model. Comparison of Figs. 3 and 4 clearly demonstrates an improvement of partitioning of surface fluxes. For instance, for the 12-h period, bias in sensible heat flux has reduced to 13.3 W m^{-2} for the stand-alone model, as compared with −35.0 W m^{-2} for the control run and −100.2 W m^{-2} for the coupled model (Table 3). This result suggests that underestimation of net radiation is a key contributing factor for the underperformance of the coupled model. It turns out that in this case the coupled model overestimates the surface temperature, which caused an excessive loss of upward longwave radiation from the land surface.

In addition, there are very small differences between the model simulation results over the FIFE-area (15 km × 15 km)- and the entire-domain (205 km × 205 km)-averaged quantities (figures not shown). This result indicates that the spatial variations of the simulated fields may not be very heterogeneous at the model grid level. An implication of this lack is that the FIFE-averaged dataset may be used to detect systematic errors in large-scale model outputs. In fact, Betts and Ball (1993) have used FIFE 1987 data to detect systematic differences in ECMWF model output.

5. Summary and discussion

Three cloud-free days are simulated from the FIFE 1987 using progressively smaller surface soil moisture

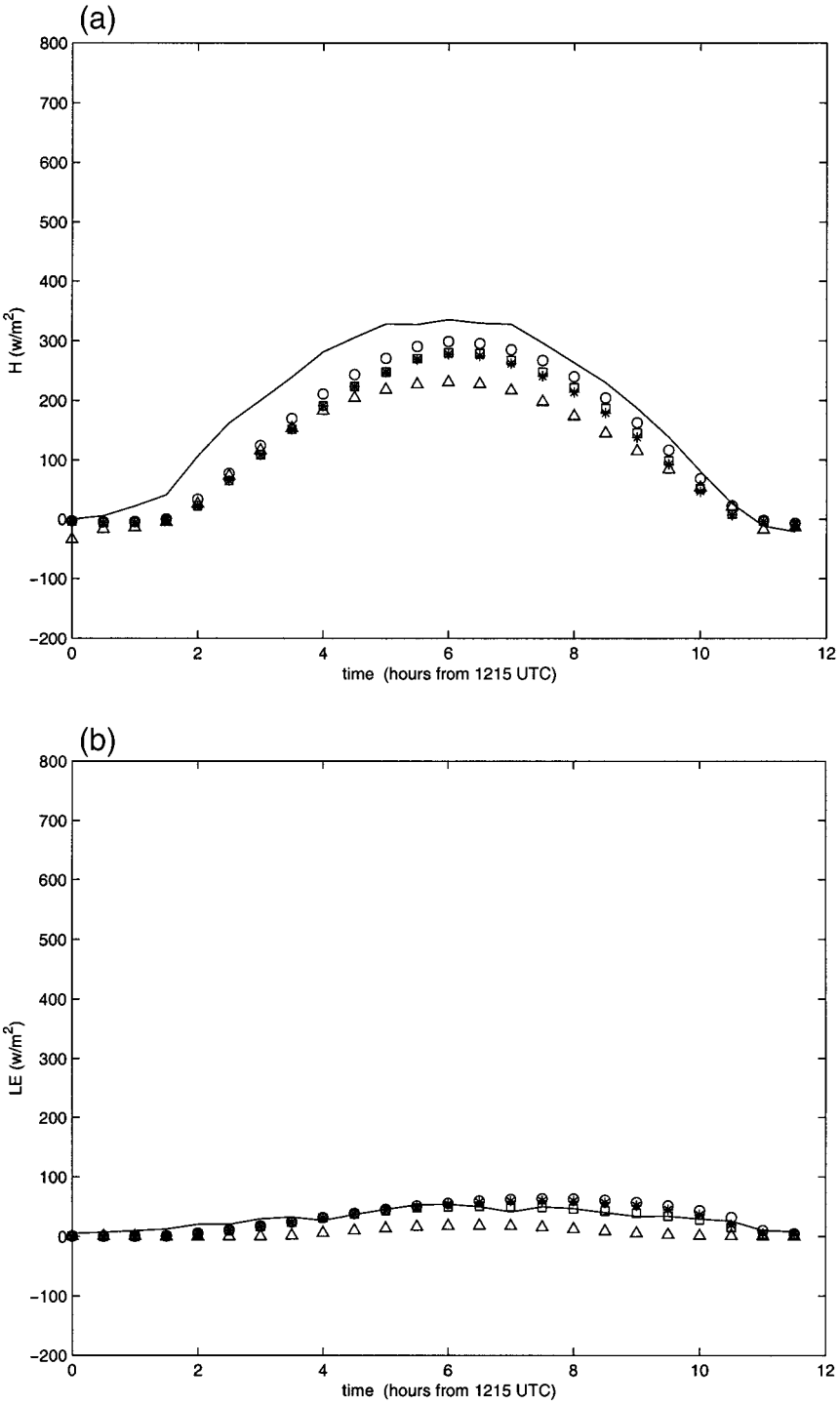

FIG. 3. (a) Sensible and (b) latent heat fluxes for 12-h simulation starting at 0600 LT 11 Oct 1987. Symbols are defined as in Fig. 1.

conditions to identify the influence of interactive soil moisture on surface flux partitioning at the diurnal timescale. A state-of-the-art atmospheric model (MM5) is used as a control run in which soil moisture is prescribed as a moisture availability function. For each day, three different representations of the soil moisture availability function are used to simulate three control simulations. In a coupled-model simulation, MM5 is coupled with a detailed land surface model.

Our preliminary results suggest that, for days with

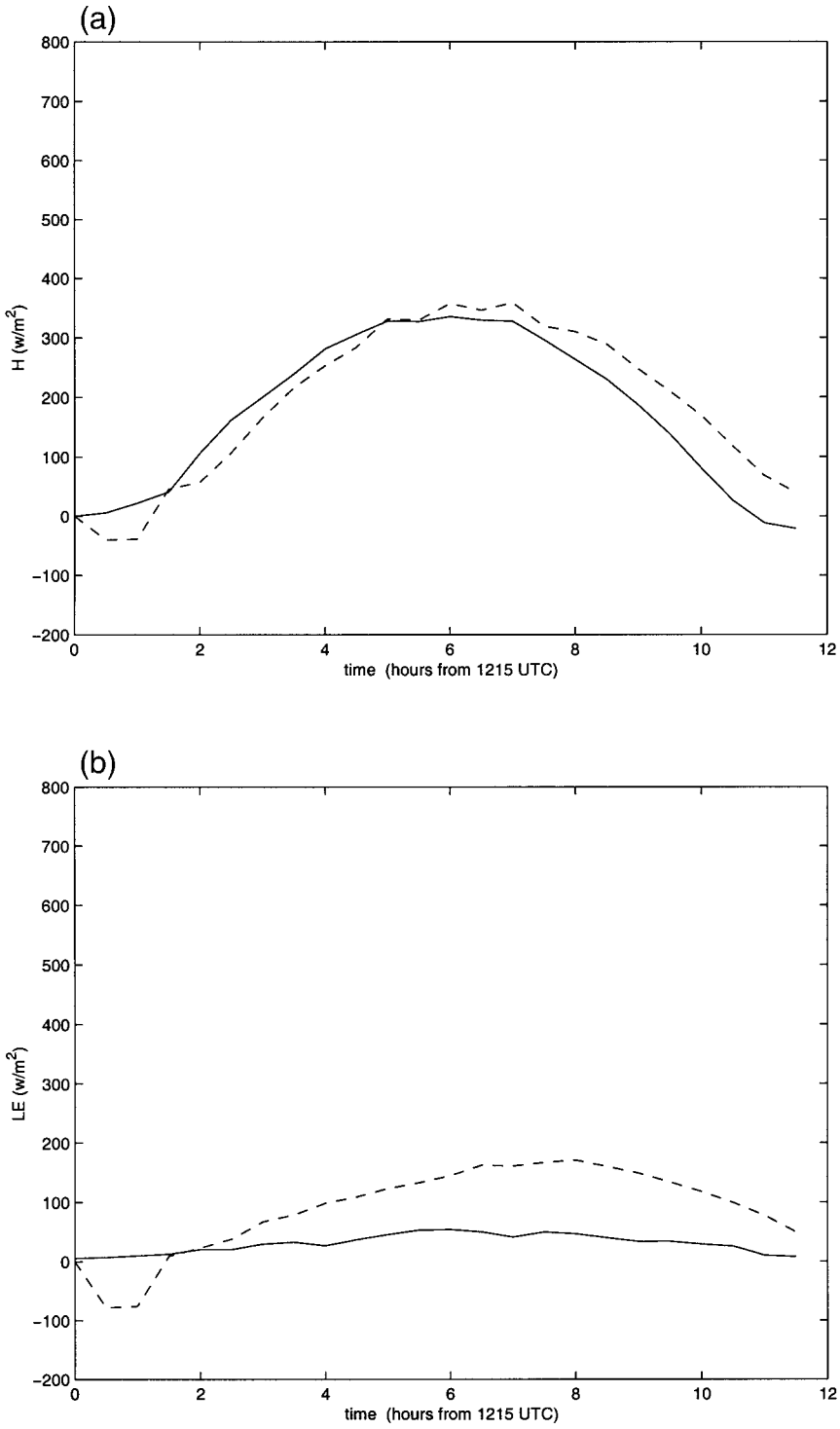

FIG. 4. (a) Sensible and (b) latent heat fluxes for 12-h simulation starting at 0600 LT 11 Oct 1987. Solid line is FIFE observation and dashed line is stand-alone ECMWF land surface model.

wetter surface soil moisture conditions and moderately high wind speed, a time-variant interactive soil moisture representation provides a more accurate partitioning of surface fluxes. It appears that a time-variant soil moisture availability function used in control-3 simulations cannot produce accurate partitioning of surface fluxes for wetter surfaces. Our results suggest that for two days, 15 August and 11 July, with initial surface soil moisture

in excess of 75% of the porosity, the coupled model simulates the temporal sequence of latent heat flux significantly better than control-run simulations in which soil moisture is represented by a time-invariant or time-varying moisture availability function.

Note that, on these two days, surface wind was also strong ($\sim$8 m s^{-1}). Previous studies have suggested that as the synoptic forcing becomes stronger the influence of mesoscale surface heterogeneities may not be as important (Dalu et al. 1996). In other words, it is argued that higher wind speed (>5 m s^{-1}) would sweep away most of the effects of small-scale heterogeneities. Our preliminary results, however, suggest that, despite moderately high wind speed for these two days, a coupled-model simulation yields a more accurate partitioning of surface fluxes. This result is partly because wind speed partially determines the turbulence at the surface and the degree of land–atmosphere coupling through the partitioning of surface fluxes. Also, a wetter surface leads to enhanced evaporation, which subsequently leads to increased moist static energy in the planetary boundary layer. This increased moist static energy may sustain and enhance turbulent transfer processes that otherwise would be swept away by stronger wind speed. On the other hand, for drier-surface states as in the case of 11 October, the depletion rate of soil moisture over a diurnal cycle is very slow, and the soil moisture states may be treated as a constant. In other words, under such conditions soil moisture representation is not very sensitive for surface flux partitioning, and a time-invariant soil moisture availability function may be adequate. We must note, however, that on this day wind speed was relatively low. Thus, it is difficult to isolate the relative influence of soil wetness and wind speed from the case studies presented here. Additional work is needed to study systematically the relative role of soil wetness and wind speed for the partitioning of surface fluxes.

To illustrate the effect of a drydown rate of soil moisture on the surface fluxes, we now examine the parameterization of surface fluxes. In the FIFE area, about 85% is covered by vegetation. Thus, the evaporation from vegetation, as shown in Eqs. (4)–(8), dominates the total evaporation. From Eq. (8) we notice that, for a very dry condition when the average soil moisture of the top and second soil layers is close to its wilting point ($\overline{\theta} \approx \theta_{\text{pwp}}$), the value of $1/f_2(\overline{\theta})$ approaches zero, which results in reduced evaporation. For such a case, the soil moisture will be almost invariant with time because of lack of evaporation. In such a case, the soil properties are not important, because the fraction $1/f_2(\overline{\theta}) = (\overline{\theta} - \theta_{\text{pwp}})/(\theta_{\text{cap}} - \theta_{\text{pwp}})$ would approach zero, irrespective of soil texture. In other words, although the sensitivity of a_L [Eq. (4)] increases when soil moisture decreases and approaches the wilting point, its influence on overall partitioning of surface fluxes is still low. This lack of influence is partly because, when soil moisture is close to the wilting point, evaporation is so low that it does not significantly affect the overall partitioning of surface fluxes. However, if the initial soil moisture is high, $\theta_{\text{cap}} - \theta_{\text{pwp}}$ [in Eq. (8)] plays an important role in estimating evaporation; that is, in such cases soil texture would also play an important role.

In summary, our preliminary results suggest that, for simulating the diurnal cycle when the land surface soil moisture and wind speed are moderately high, a detailed coupling of land surface model and atmospheric model may provide a more accurate partitioning of surface fluxes. On the other hand, for drier surface conditions with low wind speed, the use of a soil availability function instead of a detailed coupled land–atmosphere may be adequate to simulate surface fluxes accurately. An implication of this finding is that a binary switch may be implemented in a coupled land–atmosphere model that can be turned on or off based on surface soil moisture and wind conditions. For instance, for drier soil moisture conditions and low wind speed this switch would be off, and a simple moisture availability function would be adequate instead of a computationally demanding multiple–soil layer representation.

Results presented in this study should be viewed as tentative because they were obtained from only a few cloud-free days with a small range of wind speed. Thus, additional experiments are needed with more days and varying wind and surface moisture conditions. Nevertheless, our use of three different representations of a soil moisture availability function provides an understanding of the relative merits of a moisture availability function and interactive soil moisture dynamics to simulate surface flux partitioning accurately over a diurnal timescale.

Acknowledgments. Comments and suggestions from anonymous reviewers and the editor are gratefully acknowledged. This research was supported, in part, by the NASA Earth System Science Fellowship and by National Science Foundation Grant NSF9526628.

REFERENCES

Abramopoulous, F., C. Rosenzweig, and B. Choudhury, 1988: Improved ground hydrology calculation for global climate models (GCMs): Soil water movement and evapotranspiration. *J. Climate*, **1,** 921–941.

Anthes, R. A., and T. T. Warner, 1978: Development of hydrodynamical models suitable for air pollution and other mesometeorological studies. *Mon. Wea. Rev.*, **106,** 1045–1078.

Betts, A. K., and J. I. Ball, 1993: Comparison between the land surface response of the ECMWF model and the FIFE-1987 data. *Quart. J. Roy. Meteor. Soc.*, **119,** 975–1001.

Bougeault, P., B. Bret, P. Lacarrere, and J. Noilhan, 1991: An experiment with an advanced surface parameterization in mesobeta-scale model. Part II: The 16 June 1986 simulation. *Mon. Wea. Rev.*, **119,** 2374–2392.

Carlson, T. N., and F. E. Boland, 1978: Analysis of urban–rural canopy using a surface heat flux/temperature model. *J. Appl. Meteor.*, **17,** 998–1013.

Clapp, R. B., and G. M. Hornberger, 1978: Empirical equations for some hydraulic properties. *Water Resour. Res.*, **14,** 601–604.

Dalu, G. A., R. A. Pielke, M. Baldi, and X. Zeng, 1996: Heat and

momentum fluxes induced by thermal inhomogeneities with and without large-scale flow. *J. Atmos. Sci.,* **53,** 3286–3302.

Deardorff, J. W., 1977: A parameterization of ground-surface moisture content for use in atmospheric prediction models. *J. Appl. Meteor.,* **16,** 1182–1185.

——, 1978: Efficient prediction of ground-surface temperature and moisture with inclusion of a layer of vegetation. *J. Geophys. Res.,* **83,** 1889–1903.

Dudhia, J., 1993: A nonhydrostatic version of the Penn State–NCAR Mesoscale Model: Validation tests and simulation of an Atlantic cyclone and cold front. *Mon. Wea. Rev.,* **121,** 1493–1513.

Giorgi, F., and M. R. Marinucci, 1996: An investigation of the sensitivity of simulated precipitation to model resolution and its implications for climate studies. *Mon. Wea. Rev.,* **124,** 148–166.

Grell, G. A., 1993: Prognostic evaluation of assumptions used by cumulus parameterizations. *Mon. Wea. Rev.,* **121,** 764–787.

Horton, R. E., 1933: The role of infiltration in the hydrologic cycle. *Trans. Amer. Geophys. Union,* **14,** 446–460.

Hu, Z., and S. Islam, 1995: Prediction of ground surface temperature and soil moisture content by the force–restore method. *Water Resour. Res.,* **31,** 2531–2539.

Kondo, J., and N. Saigusa, 1990: A parameterization of evaporation from bare soil surface. *J. Appl. Meteor.,* **29,** 385–389.

Li, J., and S. Islam, 1999: Estimation of soil moisture profile and surface fluxes partitioning from sequential assimilation of surface layer soil moisture. *J. Hydrol.,* **220,** 86–103.

Manabe, S., 1969: Climate and the ocean circulation: The atmospheric circulation and the hydrology of the earth's surface. *Mon. Wea. Rev.,* **97,** 739–774.

McCumber, M. C., and R. A. Pielke, 1981: Simulation of the effects of surface fluxes of heat and moisture in a mesoscale numerical model. Part I: Soil layer. *J. Geophys. Res.,* **86,** 9929–9938.

Namias, J., 1958: Persistence of mid-tropospheric circulations between adjacent months and seasons. *Rossby Memorial Volume,* Rockefeller Institute Press and Oxford University Press, 240–248.

Noilhan, J., and S. Planton, 1989: A simple parameterization of land surface processes of meteorological models. *Mon. Wea. Rev.,* **117,** 536–549.

Oncley, S. P., and J. Dudhia, 1995: Evaluation of surface fluxes from MM5 using observations. *Mon. Wea. Rev.,* **123,** 3344–3357.

Pan, Z., M. Segal, R. Turner, and E. Takle, 1995: Model simulation of impacts of transient surface wetness on summer rainfall in the United States Midwest during draught and flood years. *Mon. Wea. Rev.,* **123,** 1575–1581.

Patterson, K. A., 1990: Global distribution of total and total-available soil water holding capacities. M.S. thesis, Dept. of Geography, University of Delaware, 119 pp.

Pielke, R. A., 1984: *Mesoscale Meteorological Modeling.* Academic Press, 612 pp.

Pleim, J. E., and A. Xiu, 1995: Development and testing of a surface flux planetary boundary layer model for application in mesoscale models. *J. Appl. Meteor.,* **34,** 16–32.

Sellers, P. J., 1985: Canopy reflectance, photosynthesis and transpiration. *Int. J. Remote Sens.,* **6,** 1335–1372.

Viterbo, P., and A. Beljaars, 1995: An improved land surface parameterization scheme in the ECMWF model and its validation. *J. Climate,* **8,** 2716–2748.

Warrilow, D. L., A. B. Sangster, and A. Slingo, 1986: Modeling of land-surface processes and their influence on European climate. Dynamic Climatology Tech. Note 38, The Met. Office, 92 pp.

Wood, E. F., 1991: Global scale hydrology: Advances in land surface modeling. *Rev. Geophys.,* **29** (Suppl.), 193–201.

Yang, Z. L., R. E. Dickinson, A. Henderson-Sellers, and A. J. Pitman, 1995: Preliminary study of spin-up processes in land-surface models with the first stage data of PILPS phase 1(a). *J. Geophys. Res.,* **100,** 553–578.

Yeh, T.-C., R. T. Wetherald, and S. Manabe, 1984: The effect of soil moisture on the short-term climate and hydrology change—a numerical experiment. *Mon. Wea. Rev.,* **112,** 474–490.

Zhang, D.-L., and R. A. Anthes, 1982: A high-resolution model of the planetary boundary layer—sensitivity tests and comparisons with SESAME-79 data. *J. Appl. Meteor.,* **21,** 1594–1609.

Zobler, L., 1986: A world soil file for global climate modeling. NASA Tech. Memo. 87802, 33 pp. [Available online at http://daac.gsfc.nasa.gov/CAMPAIGN_DOCS/ISLSCP/DATASET_DOCUMENTS/SOILS.html.]